Experimental Evaluation of User's Finger Effects on a 5G Terminal Antenna Array at 26 GHz

T. Q. Khai Nguyen, *Student Member, IEEE*, Md Suzan Miah, *Student Member, IEEE*, Leonardo Lizzi, *Member, IEEE*, Katsuyuki Haneda, *Member, IEEE*, Fabien Ferrero, *Member, IEEE*

***Abstract*—This paper presents the experimental evaluation of the effects of the user's fingers on the performance of a 5G terminal antenna array operating in the European 5G regulated band at 26 GHz. Matching and radiation characteristics of a four-element linear array constituted by aperture-coupled elements integrated into the mobile terminal are measured. The terminal casing and different configurations of the fingers of the user holding the terminal are considered. The obtained results indicate that the designed four-element antenna array realised the expected beamforming gain even with the perturbations by casing and user's finger, except certain finger configurations.**

***Index Terms*—array antenna, 5G, PCB, finger effects, casing effects.**

I. Introduction

The Fifth Generation Communication (5G) is announced to be officially commercialized in 2020. For the first time, millimeter wave (mmW) frequencies are introduced to mobile phone communication. Although a single resonator at mmW has very small size thanks to small electrical wavelength, antenna arrays are norm for both base station (BS) and User Equipement (UE) to achieve a sufficient signal-to-noise-ratio (SNR) to compensate higher propagation loss at mmW. A significant research effort has been conducted to characterize propagation environment at mmW as well as in the design of the BS antennas [1], [2]. However, design and characterization of UE antennas at mmW got considerably less attention compared to the studies of pathloss and BS antennas. There are many challenges involved in the design of mmW terminal antennas that have to be addressed carefully [3]. More specifically, due to the limited size of the mobile phone, antennas will be in a close proximity of nearby objects, such as the cover of the UE. As the cover will be in the near-field (NF) region of the antenna module, it will affect the antenna radiation performance [4], [5]. The effects of casing on the radiation performance of the UE antennas' have been presented in [6], [7]. A gain reduction of 3.5 dB due to metal casing is reported in [6] for high directivity antenna array at 39 GHz. The paper [7] studied the effect of casing in terms of radiation efficiency and reports a reduction ranging from 4.6% to 8.3% depending on different types of antennas at 28 GHz. Therefore, at mmW, the cover effect should be included in the study of antenna radiation characteristics. For example, coverage efficiency is one of the important metrics to characterize antenna radiation performance, which is defined by the ratio of the solid angle that UE can cover to the total 3D spherical coverage. Another important concern comes from the user's hand and body, which are also in the NF of the antenna and that can effect the antenna performance significantly. In addition, measurement-based study of antenna-human interaction is very limited because of challenges in a measurement setup and lack of reliable human phantoms at mmW. In most antenna measurement setups, Device Under Test (DUT) is mounted on a 2 axis of rotation platform in front of a reference probe [8]. A test with a real human requires otherwise a reference probe moving around a fixed DUT for the sake of high stability and repeatability.

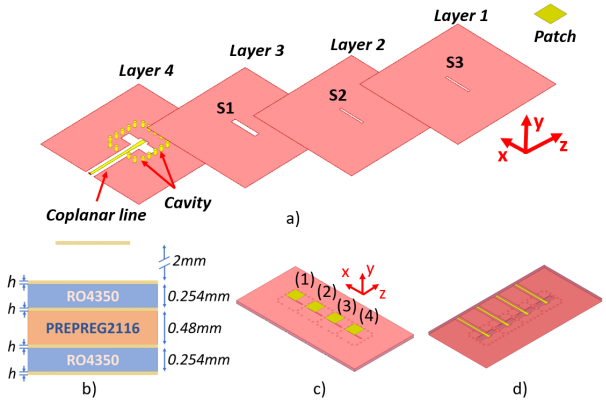

Fig. 1. Single element antenna structure. a) Separated views of different layers of the design. b) Substrate specifications and patch. c) Top view with array element placements. d) Bottom view.

The human's body effect on antenna radiation characteristics draws more attention recently and has been reported in [6], [9]–[12]. Mostly, those effects are reported in terms of losses in spherical coverage or in gain. In [9], simulations show up to 20 dB of gain reduction when a finger is placed in the NF of a patch antenna array working at 28 GHz. The work in [10] shows that human shadowing can cause a $20-25$ dB of reduction of the received power and 30% decrease in spherical coverage at 15 GHz. Those effects could also hold at higher mmW frequencies. Especially in [12], Syrytsin et al. have statistically studied the human shadowing effects of the user on performance of UE antenna array at 28 GHz through far-field measurements. However, for an accurate measurement, the probe antenna has to be sufficiently separated from the DUT. The sufficient separation distance is significantly larger when user holds antennas than antennas in free-space as the equivalent dimension of radiation source becomes larger due to scattering on a body. In contrast, near-field measurement

The work of Md. Suzan Miah and K. Haneda was supported by the Academy of Finland Research Project "Massive MIMO: Advanced Antennas, Systems and Signal Processing at mm-Waves (M3MIMO)," decision #288670.

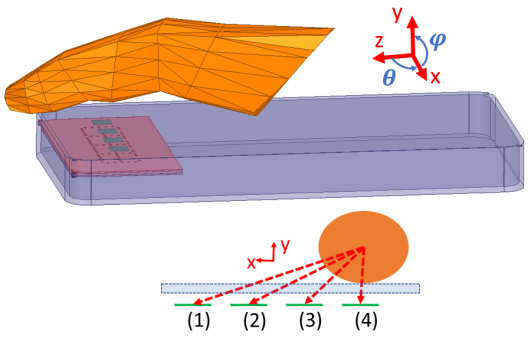

Fig. 2. The simulation of array antenna with casing and finger (top) and the illustration of distances and angular positions of coverage of the finger to array elements (bottom).

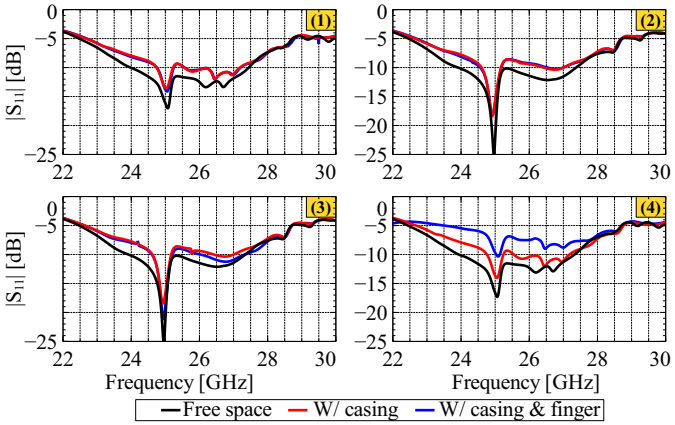

Fig. 3. Reflection coefficients of single-antenna elements.

provides a better accuracy and reliability, such as in [10]. Nevertheless, in the mentioned works, only the whole body is experimentally considered. The finger effect has never been reported separately in measurements due to the discussed measurement setup limitation. In fact, depending on the UE antenna types, the blockage of user's finger can be more severe than the shadowing by whole body [9], [13].

This paper resolves for the first time shed lights on radiation performance of antenna arrays for UE at mmW *experimentally* in the presence of casing and finger. This is made possible by using a near-field three-axis spherical measurement setup of an antenna array [14]. Effects of real human's fingers on radiation characteristics of an antenna array are studied through spherical coverage where beamforming is incorporated.

A PCB-based aperture-coupled array antenna is first shown in the next Section. The numerical models of a mobile handset together with a finger are presented in Section II. The effects of casing and user's fingers on the performance of each antenna element will be analyzed from these numerical results. Then in Section III, realized gain patterns of a prototype array operating at 26 GHz are measured using the mentioned spherical setup to confirm observations from numerical simulations. A 5-bit phase shifting is applied to the array for beamforming. Conclusions of the study are given in the final Section.

II. Array Antenna Design and Simulations

A. Antenna and array models

The antenna element constituting the array is based on the aperture-coupled structure first introduced in [15]. Taking into account the possibility of a later all-in integration, this design is realized with multiple dielectric and conductive layers based on industrial PCB stack-up as illustrated in Fig. 1a) and b). PCB technology gives antenna designer the advances in the industrial automatic procedure with high precision and mass fabrication availability. From top to bottom layers of the PCB, the three substrate materials are RO4350 ($\epsilon_r = 3.66$), pregreg 2116 ($\epsilon_r = 3.96$) and RO4350 with 0.254 mm, 0.48 mm, and 0.254 mm thick, respectively, where ϵ_r denotes relative permittivity. All copper layers are 18 μm thick. The design consists of three slots S_1, S_2 and S_3 cut in the three upper conductive layers of dimensions 5.4×0.4 mm^2, 5.4×0.4 mm^2 and 5.6×1 mm^2. A 3-mm open-ended stepped-size stub is put in the lowest conductive layer below the slots to excite an electromagnetic wave through the dielectric layers. A 4×4 mm^2 patch is placed 2 mm above the upper slot introducing an additional resonance. This allows the single element bandwidth and gain to be increased. The single-element $S_{11} \leq -10$ dB impedance bandwidth is from 24.25 to 27.5 GHz, thus covering the 5G NR FR2 band in Europe. A linear array with 4 elements is numerically modeled for optimization as depicted in Fig. 1c) and d). The distance between every two neighboring elements is $0.7\lambda_0$, where λ_0 being the wavelength in free-space at 26 GHz. Antenna elements are isolated from each other by a rectangular cavity made of vias in each element as shown in Fig 1a), where the distance between two nearby vias is 1.5 mm.

In addition to the antenna array, the casing and the finger are also modeled. The casing is made of Acrylonitrile Butadiene Styrene (ABS), a commonly-used material for 3D printing with $\epsilon_r = 2.5$. Its volume covers $50 \times 100 \times 10$ mm^3 and the thickness is 1 mm for all the surfaces. The surface of the casing towards the $-y$ direction is modeled as a finite conductivity sheet, representing the handheld terminal screen. A model of the finger is also added. Interestingly, the human skin at a higher frequencies has higher conductivity and lower permittivity, which leads to lower penetration depth of around 1 mm [16]. Thanks to this feature, it is sufficient to consider an electrically homogeneous simulation model of a human body at mmW representing only the skin. The finger is created with homogeneous properties with $\epsilon_r = 17.71$ and conductivity $\sigma = 24.41$ S/m which are extracted from Gabriel model of dry skin at 26 GHz [17]. The antenna array is positioned with respect to the casing and the finger as shown in Fig. 2. The minimum distance between the antennas and the casing is 0.6 mm. The finger is outside the casing tilted by 12° with respect to the z-axis on xOz plane and being centered above the fourth element.

B. Matching and realized gains

Fig. 3 illustrates the impedance matching of all the array elements with presence and absence of a finger and casing. All the elements achieve $|S_{11}| \leq -10$ dB reflection coefficient over the band of interest in free-space. The casing causes a worse matching, with the maximum $|S_{11}|$ increased up to -7.5

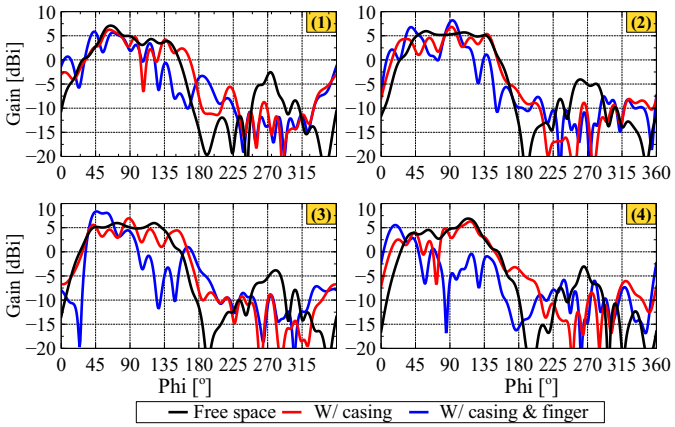

Fig. 4. Simulated realized gains of single-antenna elements at 26GHz on azimuth plane.

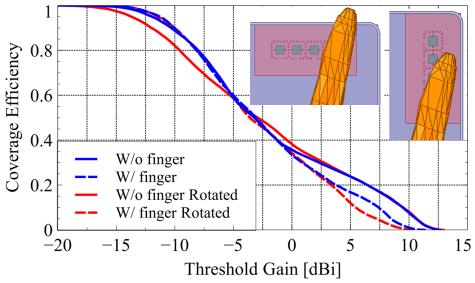

Fig. 5. Simulated coverage efficiencies for two different orientations of the patch array (to study the impact of the finger in two orthogonal polarization cases).

dB in the same band, as shown in red curve. All the array elements equally suffer from this effect. The presence of the finger, on the contrary, causes the worsening of the impedance matching only on the fourth element, i.e., the one closer to the finger. However, the $|S_{11}|$ is still lower than -6 dB, which is acceptable for UE antennas. Besides, the isolation between elements is also impacted, where the worst isolation is 23 dB in free space, 18 dB with the casing and 15 dB with the casing and finger.

As mentioned in Sect. I, any object inside the near-field region will impact not only the impedance matching but also the gains of the antenna elements. As shown in Fig. 4, all the elements have a simulated realized gain higher than 5 dB and a half-gain beamwidth wider than 70°, centered at $\phi = 90°$. By adding the casing, the gain patterns of all the elements fluctuate. There are even some blind angles at around $\phi = 102°$ and $\phi = 78°$, where 8 dB of attenuation is observable, for the first and fourth elements, respectively, probably caused by the scattering of the waves on the casing. The effect of the presence of the finger in terms of antenna gains can be clearly seen in Fig. 4 on the blue curves. The constructive and destructive interference due to the scattering from finger surface can be observed on the radiation pattern as a lower main lobe and higher side lobe levels. For example, there is attenuation in best/worst case of 7/20 dB within $120° \leq \phi \leq 150°$ for the gain of the third element, while 4 dB is added up at $\phi = 50°$. The same effects are reported by simulations in [9] at both 28 GHz and 60 GHz. At 28 GHz, the levels of attenuation and increase in radiation to side and back angles agree well with this work.

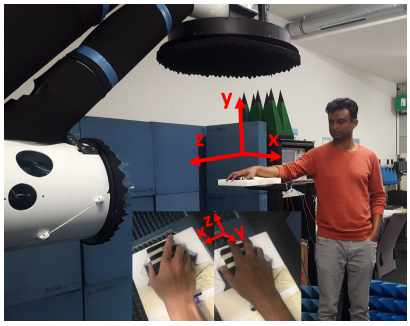

Fig. 6. Radiation measurement with real human's hand using spherical scanner. 1-finger (left) and 2-finger (right) configurations are represented in the small figure at the bottom.

C. Coverage Efficiency

Each antenna element is assumed to be fed with a 5-bit phase-shifter, which supports 11.25° phase step. Starting from the gain patterns of antenna elements in the array, beam patterns of the array is synthesized by applying all the possible phase shifts to the element gain patterns and successively summing up all the resulting vector pattern configurations, as reported in [18].

As stated in [19], conventional parameters like total radiated power (TRP) or total isotropic sensitivity (TIS) are less effective in characterizing beam steering capability of a UE. In this work, the coverage efficiency is evaluated [4], [5] as a figure-of-merit measuring the power radiated toward a specific direction. The metric is calculated from synthesized beam pattern, or total scan gain pattern, and can be presented as a cumulative distribution function (CDF) of the gain threshold (Fig. 5, blue curves).

In order to analyze the effect of the finger also in the orthogonal polarization case, the model in which the patch array is rotated to be perpendicular to the shorter edge of the mobile terminal has been simulated. The results are added to Fig. 5 in red. As it can be noticed, the finger gives almost similar losses at gain thresholds higher than 0 dBi for both the polarizations, though there are some small differences in term of gain level. These losses can be as high as 3 dB in first mentioned case and 5 dB in rotated case.

III. Antenna Array Measurements

A. Single element measurements

The effects of the user's finger on the antenna gain have been experimentally evaluated. The gain measurements have been performed for a single frequency at 26 GHz where the measured $|S_{11}|$ is lower than -9 dB for all the elements. A three-axis spherical near field scanner is used to enable measurements with a human being. In this setup, a robot arm moves the probe over the surface of a sphere centered on a fix DUT. This mechanism allows a person to place his/her hand over the DUT during the measurement, as shown in Fig. 6 and previously reported in [20], [21].

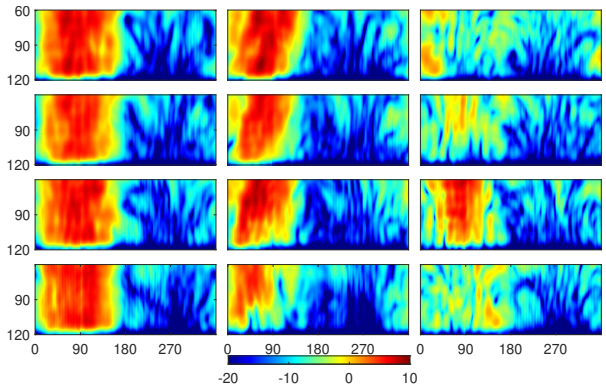

Fig. 7. Realized gains of each antenna element in the array for three cases of finger intervention. In each sub-figure, θ and ϕ [°] are shown in vertical and horizontal directions, respectively.

The antenna gain is first measured in free space with casing for $-150^\circ \leq \theta \leq 150^\circ$ due to DUT holder blockage. Two typical finger placements on the casing have been chosen for the measurements. In the first one, the finger mimics the position of the finger used in simulations. The index finger is covering the fourth element. The second case is chosen to illustrate a user covering the antenna array with two fingers. In this case, the index finger is placed between the first and the second element, while the middle finger covers the fourth element.

Figure 7 shows the realized gains of each antenna element, where the i^{th} row corresponds to element i. The first, second and third columns in the figure corresponds to cases without the hand, with one finger and with two fingers, respectively. Because the maximum radiation of each element is in the direction at $\theta = 90^\circ, \phi = 90^\circ$, the polar angular range is limited to $60^\circ \leq \theta \leq 120^\circ$ in the plot. The effect of the finger in the one-finger case is clearly observable on the fourth antenna element. The realized gain suffers from stronger distortion while the remaining elements of this case are less affected by the presence of the finger, confirming the numerical results. In the two-fingers case, the appearance of reflected and diffracted fields from the fingers can be seen in side and back angles. The radiation from elements 1, 2 and 4 is reduced and the third element still maintains gain levels as in free-space.

B. Beamforming and coverage efficiency

Figure 8 (left) illustrates the maximum gain of synthesized beam patterns over azimuth angles for the aforementioned three cases of finger intervention to the antenna array. The differences of synthesized beam pattern in the azimuth plane are clearly observable.

The estimated coverage efficiency at 26 GHz in Figure 8 (right) shows that the realized gain of the array in the one-finger case has a constant loss of up to 5 dB of gain compared to the case without the finger. Nevertheless, the achieved maximum gain is about 13 dBi in both cases. The measured gains of our antenna array with casing are in agreement with those reported in [22] using a similar antenna structure. The antenna array in this work, however, differs for the ABS material of the casing and the thickness of the structure.

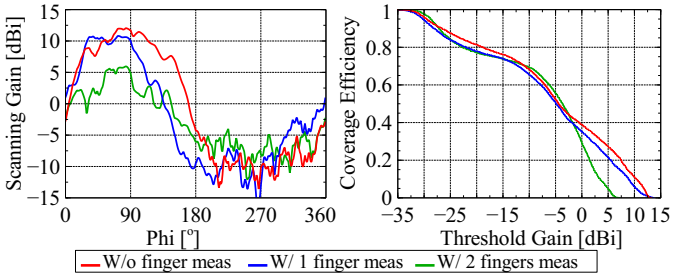

Fig. 8. Maximum gain across azimuth angles (left) and coverage efficiency (right) of array antenna in different cases.

In the two-finger case, the maximum gain reduces to about 6 dBi, similarly to the gain when only one element is activated, indicating that almost no beamforming gain is obtained . Only the third element, i.e., the one not being covered by the fingers, is effectively contributing to the radiation.

Very similar results (not reported here) are obtained at different frequencies within the 24-28 GHz band. The maximum variation of the threshold gain over the entire band is $\pm$ 1.5 dBi. Furthermore, since glass is widely used as smartphone cover material, the spherical coverage efficiency with finger effect using an industrial glass casing with $\epsilon_r = 6.84$ [23] at 26 GHz and 1 mm thickness has been simulated. The higher permittivity of glass is inducing more scattering. Coverage efficiency for gain threshold higher than 5 dBi is reduced by 67% compare with ABS.

IV. Conclusion

In this paper, the near-field effects of the user's finger on the performance of a 5G mobile terminal antenna working in the European 5G NR band at 26 GHz (band n258) have been experimentally evaluated. Towards this end, a linear array of four aperture-coupled antenna elements compatible with current multi-layer PCB technology has been designed. A prototype including the terminal casing has been fabricated for measurements. Both single-element and synthesized beam patterns of the array have been measured considering multiple configurations of the user's finger covering the array elements. It must be pointed out that all the reported measurements are in well agreement with the numerical data.

Measurements have shown that the single-element antenna gain can be reduced up to 20 dB in certain directions because of the shadowing from the user's finger. However, the array is still able to maintain the spherical coverage efficiency using beamforming in the one-finger case. In the two-finger case, the realized gains are severely reduced even with beamforming, thus causing a strong reduction of the radio link performance. The same results have been obtained by substituting the broadside antenna array considered in this paper with the end-fire array presented in [18]. This demonstrates that the position of the hand on the terminal, and consequently the number of array elements that are covered by the fingers, are more important than the geometry of the array element itself. Implementing sub-arrays at different position in the terminal is a necessary solution to mitigate finger shadowing effects and to increase the coverage.

REFERENCES

[1] K. R. Mahmoud and A. M. Montaser, "Performance of Tri-Band Multi-Polarized Array Antenna for 5G Mobile Base Station Adopting Polarization and Directivity Control," *IEEE Access*, vol. 6, pp. 8682–8694, 2018.

[2] T. S. Rappaport, S. Sun, R. Mayzus, H. Zhao, Y. Azar, K. Wang, G. N. Wong, J. K. Schulz, M. Samimi, and F. Gutierrez, "Millimeter Wave Mobile Communications for 5G Cellular: It Will Work!," *IEEE Access*, vol. 1, pp. 335–349, 2013.

[3] Y. Huo, X. Dong and W. Xu, "5G Cellular User Equipment: From Theory to Practical Hardware Design," *IEEE Access*, vol. 5, pp. 13992–14010, 2017.

[4] I. Syrytsin, S. Zhang and G. F. Pedersen, "User Impact on Phased and Switch Diversity Arrays in 5G Mobile Terminals," *IEEE Access*, vol. 6, pp. 1616–1623, 2018.

[5] I. Syrytsin, S. Zhang, G. F. Pedersen, and Z. Ying, "User Effects on the Circular Polarization of 5G Mobile Terminal Antennas," *IEEE Trans. Ant. Propag..*, vol. 66, no. 9, pp. 4906–4911, Sep. 2018.

[6] I. Syrytsin, S. Zhang and G. F. Pedersen, "Effects of Phone Case and User Effects on Switched-Beam High Gain Antenna System for 5G Mobile Terminals," *Int. Conf. on Electromag. Advanced Applications (ICEAA)*, Cartagena des Indias, 2018, pp. 110–113.

[7] B. Xu, Z. Ying, L. Scialacqua, A. Scannavini, L. J. Foged, T. Bolin, K. Zhao, S. He, and M. Gustafsson, "Radiation Performance Analysis of 28 GHz Antennas Integrated in 5G Mobile Terminal Housing," *IEEE Access*, vol. 6, pp. 48088–48101, 2018.

[8] C.A. Balanis, C. R. Birtcher, "Antenna Elements", in *Modern Antenna Handbook*, Wiley, 2008, pp. 977–1033.

[9] M. Heino, C. Icheln, and K. Haneda, "Self-user shadowing effects of millimeter-wave mobile phone antennas in a browsing mode," in *13th European Conf.on Ant. and Propag. (EuCAP 2019),* pp. 1–5, Mar.-Apr. 2019.

[10] K. Zhao, J. Helander, D. Sjöberg, S. He, T. Bolin, Z. Ying, "User Body Effect on Phased Array in User Equipment for the 5G mmW Communication System," *IEEE Ant. Wireless Propag. Lett.*, vol. 16, pp. 864–867, 2017.

[11] B. Yu, K. Yang, C. Sim and G. Yang, "A Novel 28 GHz Beam Steering Array for 5G Mobile Device With Metallic Casing Application," *IEEE Trans. Ant. Propag..*, vol. 66, no. 1, pp. 462–466, Jan. 2018.

[12] I. Syrytsin, S. Zhang, G. F. Pedersen, K. Zhao, T. Bolin, and Z. Ying, "Statistical Investigation of the User Effects on Mobile Terminal Antennas for 5G Applications," *IEEE Trans. Ant. Propag..*, vol. 65, pp. 6596–6605, 2017.

[13] M. Heino, C. Icheln, and K. Haneda, "Finger effect on 60 GHz user device antennas," in *10th European Conf.on Ant. and Propag. (EuCAP 2016),* pp. 1–5, Apr. 2016.

[14] F. Ferrero, Y. Benoit, L. Brochier, J.Lanteri, J-Y. Dauvignac, C. Migliaccio, S. Gregson, "Spherical Scanning Measurement Challenge for Future Millimeter Wave Applications," *AMTA 2015*, Oct. 2015, Long Beach, USA.

[15] D. M. Pozar, "Microstrip antenna aperture-coupled to a microstripline," *Elect. Lett.*, vol. 21, no. 2, pp. 49–50, Jan. 1985.

[16] T. Wu, T. S. Rappaport, and C. M. Collins, "The human body and millimeter-wave wireless communication systems: Interactions and implications," in *IEEE Int. Conf. on Commun. (ICC)*, pp. 2423–2429, 2015.

[17] S. Gabriel, R. W. Lau, and C. Gabriel, "The dielectric properties of biological tissues: III. Parametric models for the dielectric spectrum of tissues," *Phys. Med. Biol. 41*, pp. 2271–2293, 1996.

[18] F. Ferrero, P. Ratajkzack, and T. Q. K. Nguyen, "Assessment of beamforming capabilities of a 4-element array in a smartphone at 26 GHz," in *12th European Conf. on Ant. and Propag. (EuCAP 2018)*, pp. 1–3, 2018.

[19] K. Zhao, S. Zhang, Z. Ho, O. Zander, T. Bolin, Z. Ying, and G. F. Pedersen , "Spherical Coverage Characterization of 5G Millimeter Wave User Equipment With 3GPP Specifications," in *IEEE Access*, vol. 7, pp. 4442–4452, 2019.

[20] C. Buey, F. Ferrero, L. Lizzi, and P. Ratajczak, "Measurement set-up for the assessment of user impact on handheld terminal beyond 10 GHz," in *IEEE Conf. Ant. Measure. and Applications (CAMA)*, pp. 327–329, 2017.

[21] C. Buey, F. Ferrero, L. Lizzi, P. Ratajczak, Y. Benoit, and L. Brochier, "Investigation of hand effect on a handheld terminal at 11 GHz," in *10th European Conf. on Ant. and Propag. (EuCAP)*, pp. 1–5, 2016.

[22] J. Helander, K. Zhao, Z. Ying, and D. Sjöberg, "Performance analysis of millimeter-wave phased array antennas in cellular handsets," *IEEE Ant. Wireless Propag. Lett.*, vol. 15, pp. 504–507, 2016.

[23] Corning, "Corning Gorilla Glass 6," Product Information Sheet, Apr. 2018 (rev. C).